

ELASTIC CONSOLIDATION AROUND A DEEP CIRCULAR TUNNEL

J. P. CARTER

Department of Civil Engineering, University of Queensland, St. Lucia, Queensland, Australia

and

J. R. BOOKER

Department of Civil Engineering, University of Sydney, Sydney, Australia

(Received 13 July 1981; in revised form 15 March 1982)

Abstract—A method of analysis is presented for the consolidation of a linear elastic soil due to the cutting of a long and deep circular tunnel. Solutions have been obtained for the time dependent displacements and stress changes occurring in the soil surrounding the tunnel opening.

NOMENCLATURE

A_1, A_2, \dots, A_6	constants
c	coefficient of consolidation
$e_r, e_{\theta\theta}$	radial and circumferential strains
e_v	volume strain
E_v	Fourier coefficient of volume strain
G	elastic shear modulus
I_n, K_n	modified Bessel Functions of order n
k	permeability coefficient
K_0	coefficient of earth pressure at rest
n	Fourier integer
N	ratio of horizontal to vertical total stress
p_0	<i>in situ</i> pore water pressure
p	excess pore pressure
P	Fourier coefficient of excess pore pressure
r	radial coordinate
r_0	radius of tunnel
s	Laplace Transform variable
t	time since tunnel cutting
u_r, u_{θ}	radial and circumferential displacements
U_r, U_{θ}	Fourier Coefficients of displacement
$S_r, S_{\theta\theta}, S_{r\theta}$	Fourier Coefficients of stress
$\gamma_{r\theta}$	shear strain
γ_w	unit weight of pore water
θ	circumferential coordinate
λ	Lamé constant for soil skeleton
ν'	Poisson's ratio for soil skeleton
σ_d	one half of the <i>in situ</i> deviator stress
σ_m	mean <i>in situ</i> total stress
$\sigma_r, \sigma_{\theta\theta}, \sigma_{r\theta}$	stress components
ϕ	deformation function
Φ	Fourier Coefficient of ϕ
ϕ_1, ϕ_2	solution functions
ψ_1, ψ_2	solution functions
ω	rotation
Ω	Fourier Coefficient of ω

1. INTRODUCTION

The problem of a tunnel in saturated clay is of some interest to geotechnical engineers concerned with the design of tunnel linings or tunnel support systems. As a first approximation the soil surrounding the tunnel is often idealised as an isotropic, elastic continuum and some solutions have been obtained for the displacements and stress changes in the elastic medium after tunnel boring, e.g. [1, 2].

In the earlier investigations the soil was considered to behave as a single phase material and hence the solutions obtained are relevant only to the short term

(or undrained) condition and the long term (or fully drained) condition. However, when an opening is created in a saturated medium the resulting displacements and stress changes will be time dependent. This time dependence arises because of the two phase nature of a saturated elastic material. Volume change can only take place as water is expelled from the voids between the solid particles. Movement of water through the soil cannot occur instantaneously and so any deformations which involve a change in volume will require a finite time in which to take place. Conversely, any deformations which involve only shearing can occur instantaneously.

In this paper solutions are presented for the displacements and stress changes around a long circular opening in a saturated elastic medium. It is assumed that the time dependence of these changes is due entirely to consolidation of elastic soil. No consideration is given to other time dependent phenomena such as creep.

2. PROBLEM DESCRIPTION

It is assumed that the tunnel will be bored at a depth which is large when compared with the nominal radius of the tunnel opening. To sufficient accuracy the *in situ* stress state in the ground, prior to tunnel cutting, may be idealised as being uniform with a total normal stress σ_v , which acts in the vertical direction, and a total normal stress σ_H , which acts in all horizontal directions. The horizontal total stress may be expressed as a proportion of the total vertical stress, thus

$$\sigma_H = N\sigma_v \quad (1)$$

The principle of effective stress gives

$$\sigma_v = \sigma_v' + p_0$$

$$\sigma_H = \sigma_H' + p_0$$

where σ_v' and σ_H' are vertical and horizontal effective stress components, respectively, and p_0 is the *in situ* pore water pressure. Compressive stress is considered to be positive. The coefficient of earth pressure at rest K_0 , is defined by

$$\sigma_H' = K_0\sigma_v' \quad (2)$$

For a soil deposit with the water table at the surface, and a bulk unit weight γ , then

$$N = K_0 - \frac{\gamma_w}{\gamma} (K_0 - 1) \quad (3)$$

where γ_w is the unit weight of water.

For the circular opening it is more convenient to express the *in situ* stress state in terms of polar coordinates, see Fig. 1. It follows that the total stresses acting on a circular boundary are given by

$$\sigma_{rr} = \sigma_m + \sigma_d \cos 2\theta \quad (4a)$$

$$\sigma_{\theta\theta} = \sigma_m - \sigma_d \cos 2\theta \quad (4b)$$

$$\sigma_{r\theta} = -\sigma_d \sin 2\theta \quad (4c)$$

where

$$\sigma_m = \frac{1}{2}(\sigma_H + \sigma_v)$$

$$\sigma_d = \frac{1}{2}(\sigma_H - \sigma_v).$$

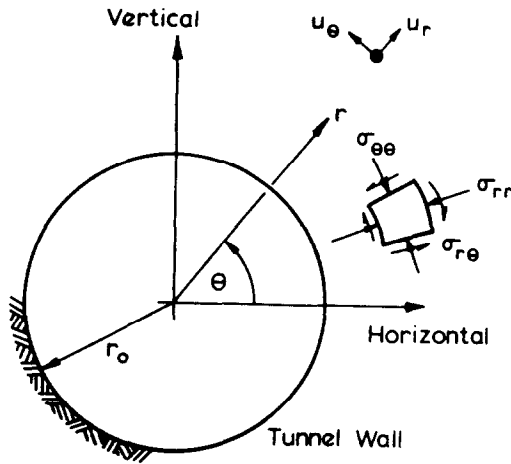


Fig. 1. Definition of tunnel problem and coordinate system.

Equations (4) give the stresses which act at the periphery of the tunnel before it is bored. After boring the normal total stress σ_{rr} and the shear stress $\sigma_{r\theta}$ are both removed from the tunnel boundary. Hence the stress boundary conditions for this problem may be idealised as

$$\Delta\sigma_{rr} = -\sigma_m - \sigma_d \cos 2\theta \quad \left. \vphantom{\Delta\sigma_{rr}} \right\} \text{at } r = r_0 \quad (5a)$$

$$\Delta\sigma_{r\theta} = \sigma_d \sin 2\theta \quad \left. \vphantom{\Delta\sigma_{r\theta}} \right\} \quad (5b)$$

where the symbol Δ indicates a change in the appropriate quantity.

It is also necessary to consider the hydraulic boundary conditions at the tunnel wall, since the soil is saturated. There are two important cases which may be identified. These are:

- (a) a permeable tunnel, and
- (b) an impermeable tunnel.

For these situations the corresponding boundary conditions are

$$(a) \quad p = 0 \text{ at } r = r_0 \quad (6a)$$

$$(b) \quad \frac{\partial p}{\partial r} = 0 \text{ at } r = r_0. \quad (6b)$$

Equations (5) and (6) describe the complete boundary conditions at the tunnel wall, which correspond to the removal of material to form a circular opening. In order to simplify the analysis, the principle of superposition is employed and the following components of the problem are considered.

(a) *Permeable tunnel*

For the permeable tunnel, three separate components may be identified. These are:

Case Ia

$$\left. \begin{aligned} \Delta\sigma_{rr} &= -\sigma_m \\ \Delta\sigma_{rr} &= 0 \\ p &= 0 \end{aligned} \right\} \text{when } r = r_0.$$

Case IIa

$$\left. \begin{aligned} \Delta\sigma_{rr} &= 0 \\ \Delta\sigma_{r\theta} &= 0 \\ \Delta p &= -p_0 \end{aligned} \right\} \text{when } r = r_0.$$

Case IIIa

$$\left. \begin{aligned} \Delta\sigma_{rr} &= -\sigma_d \cos 2\theta \\ \Delta\sigma_{r\theta} &= \sigma_d \sin 2\theta \\ p &= 0 \end{aligned} \right\} \text{when } r = r_0.$$

(b) Impermeable tunnel

For the impermeable tunnel only two non-trivial components need be considered. These are:

Case Ib

$$\left. \begin{aligned} \Delta\sigma_{rr} &= -\sigma_m \\ \Delta\sigma_{r\theta} &= 0 \\ \frac{\partial p}{\partial r} &= 0 \end{aligned} \right\} \text{when } r = r_0$$

Case IIIb

$$\left. \begin{aligned} \Delta\sigma_{rr} &= -\sigma_d \cos 2\theta \\ \Delta\sigma_{r\theta} &= \sigma_d \sin 2\theta \\ \frac{\partial p}{\partial r} &= 0 \end{aligned} \right\} \text{when } r = r_0$$

It will be demonstrated later that the solutions to Cases Ia and Ib are identical, i.e. they are independent of the hydraulic boundary conditions.

3. GENERAL SOLUTION

Using a polar coordinate system the equations for consolidation of an isotropic, elastic soil under conditions of plane strain may be written:

$$\frac{\partial\sigma_{rr}}{\partial r} + \frac{1}{r} \frac{\partial\sigma_{r\theta}}{\partial\theta} + \frac{\sigma_{rr} - \sigma_{\theta\theta}}{r} = 0 \quad (7a)$$

$$\frac{\partial\sigma_{r\theta}}{\partial r} + \frac{1}{r} \frac{\partial\sigma_{\theta\theta}}{\partial\theta} + 2 \frac{\sigma_{r\theta}}{r} = 0 \quad (7b)$$

$$\sigma_{rr} - p = -\lambda e_v - 2G e_{rr} \quad (8a)$$

$$\sigma_{\theta\theta} - p = -\lambda e_v - 2G e_{\theta\theta} \quad (8b)$$

$$\sigma_{r\theta} = -G\gamma_{r\theta}$$

where λ and G are the Lamé parameters for the elastic soil skeleton (compressive stress and compressive pore pressure are taken as positive);

$$e_{rr} = \frac{\partial u_r}{\partial r} \quad (9a)$$

$$e_{\theta\theta} = \frac{u_r}{r} + \frac{1}{r} \frac{\partial u_\theta}{\partial\theta} \quad (9b)$$

$$\gamma_{r\theta} = \frac{1}{r} \frac{\partial u_r}{\partial\theta} + \frac{\partial u_\theta}{\partial r} - \frac{u_\theta}{r} \quad (9c)$$

$$e_v = e_{rr} + e_{\theta\theta} \quad (9d)$$

$$V^2 \bar{e}_v = \frac{s}{c} \bar{e}_v \quad (10)$$

where, for the elastic soil,

$$c = \frac{k}{\gamma_w} \cdot (\lambda + 2G) = \frac{k}{\gamma_w} \cdot 2G \cdot \frac{(1 - \nu')}{(1 - 2\nu')}$$

with k = isotropic permeability coefficient; γ_w = unit weight of pore fluid; ν' = Poisson's ratio for the soil skeleton; and where u_r and u_θ are the r and θ components of displacement respectively, and the symbol “-” denotes the Laplace transform of the appropriate quantity, e.g.

$$\bar{e}_v = \int_0^\infty \exp(-st) e_v(t) dt.$$

The symbol t is used to represent the time elapsed since the instantaneous tunnel boring. In eqns (7) and (8) the symbol Δ has been omitted for convenience and σ_{rr} , $\sigma_{\theta\theta}$, $\sigma_{r\theta}$ and p are now used to represent changes in the *in situ* stress state and pore pressure due to tunnel boring. The governing equations may also be written as

$$(\lambda + 2G) \frac{\partial e_v}{\partial r} - \frac{G}{r} \frac{\partial \omega}{\partial \theta} = \frac{\partial p}{\partial r} \quad (11a)$$

$$(\lambda + 2G) \frac{1}{r} \frac{\partial e_v}{\partial \theta} + G \frac{\partial \omega}{\partial r} = \frac{1}{r} \frac{\partial p}{\partial \theta} \quad (11b)$$

$$\nabla^2 \bar{e}_v = \frac{s}{c} \bar{e}_v$$

where

$$e_v = \frac{1}{r} \frac{\partial}{\partial r} (ru_r) + \frac{1}{r} \frac{\partial u_\theta}{\partial \theta},$$

$$\omega = -\frac{1}{r} \frac{\partial u_r}{\partial \theta} + \frac{1}{r} \frac{\partial}{\partial r} (ru_\theta)$$

are the volume strain and rotation. On introducing ϕ defined by

$$p = G\phi + (\lambda + 2G)e_v$$

these equations may also be written as

$$-\frac{1}{r} \frac{\partial \omega}{\partial \theta} = \frac{\partial \phi}{\partial r} \quad (12a)$$

$$\frac{\partial \omega}{\partial r} = \frac{1}{r} \frac{\partial \phi}{\partial \theta} \quad (12b)$$

$$\nabla^2 \bar{e}_v = \frac{s}{c} \bar{e}_v \quad (12c)$$

Solutions shall be sought which have the form:

$$u_r = U_r \cos(n\theta + \epsilon) \quad (13a)$$

$$u_\theta = U_\theta \cos(n\theta + \epsilon) \quad (13b)$$

$$p = P \cos(n\theta + \epsilon) \quad (13c)$$

$$\sigma_{rr} = S_{rr} \cos(n\theta + \epsilon) \quad (13d)$$

$$\sigma_{\theta\theta} = S_{\theta\theta} \cos(n\theta + \epsilon) \quad (13e)$$

$$\sigma_{r\theta} = S_{r\theta} \sin(n\theta + \epsilon) \tag{13f}$$

$$e_\nu = E_\nu \cos(n\theta + \epsilon) \tag{13g}$$

$$\omega = \Omega \sin(n\theta + \epsilon) \tag{13h}$$

$$\phi = \Phi \cos(n\theta + \epsilon). \tag{13i}$$

Equations (12) then become

$$-\frac{n}{r} \Omega = \frac{\partial \Phi}{\partial r} \tag{14a}$$

$$-\frac{n}{r} \Phi = \frac{\partial \Omega}{\partial r} \tag{14b}$$

$$\frac{\partial^2 \bar{E}_\nu}{\partial r^2} + \frac{1}{r} \frac{\partial \bar{E}_\nu}{\partial r} - \frac{n^2}{r^2} \bar{E}_\nu = \frac{s}{c} \bar{E}_\nu \tag{14c}$$

where

$$\bar{E}_\nu = \frac{1}{r} \frac{\partial}{\partial r} (r \bar{U}_\theta) + \frac{n}{r} \bar{U}_r$$

$$\Omega = \frac{1}{r} \frac{\partial}{\partial r} (r U_\theta) + \frac{n}{r} U_r.$$

Equation (14c) is the modified Bessel equation of order n so that

$$2G \bar{E}_\nu = A_1 K_n \left(\sqrt{\left(\frac{s}{c}\right) r} \right) + A_2 I_n \left(\sqrt{\left(\frac{s}{c}\right) r} \right) \tag{14d}$$

where K_n, I_n are the modified Bessel functions of order n .

Equations (14a, b) can be reduced to linear equations with constant coefficients by the substitution $r = \exp(\zeta)$ and it follows that

$$2G \Phi = A_3 r^{-n} + A_4 r^n \tag{14e}$$

$$2G \Omega = A_3 r^{-n} - A_4 r^n. \tag{14f}$$

If we now solve eqns (14d-f) for the transforms of displacement coefficients U_r, U_θ we find that the general solution can be expressed in terms of six independent solutions:

$$\begin{bmatrix} \bar{U}_r \\ \bar{U}_\theta \\ \frac{\bar{P}}{2G} \\ \frac{\bar{S}_{rr}}{2G} \\ \frac{\bar{S}_{\theta\theta}}{2G} \\ \frac{\bar{S}_{r\theta}}{2G} \end{bmatrix} = M \begin{bmatrix} A_1 \\ A_2 \\ A_3 \\ A_4 \\ A_5 \\ A_6 \end{bmatrix} \tag{15}$$

where the terms of matrix M are given in Appendix A and the constants A_1 to A_6 may be found from the appropriate boundary conditions.

In order to recover the coefficients U_r , etc. the Laplace transforms given by eqns (15) must be inverted. This can be achieved by an application of the Complex Inversion Theorem, i.e. for

the general function $f(t)$ the inversion is given by

$$f(t) = \frac{1}{2\pi i} \int_C \tilde{f}(s) e^{st} ds \quad (16)$$

where s is a complex variable and C is any contour in the complex plane such that all singularities of $\tilde{f}(s)$ lie to the left of C .

4. SOLUTIONS FOR THE TUNNEL PROBLEM

The particular solutions for the tunnel problem, i.e. for Cases I, II and III, may be obtained from Equations (15) after insertion of the relevant boundary conditions.

Case I

For case I, $n = 0$ and $\epsilon = 0$ and thus U_θ and $S_{r\theta}$ vanish automatically. The solution which remains bounded as $r \rightarrow \infty$ consists of only two parts; solutions 1 and 5. The constants A_1 and A_5 may be obtained from the boundary conditions at $r = r_0$, and it may be shown that for both an impermeable tunnel and a permeable tunnel the solutions are identical, with

$$A_1 = 0$$

and

$$A_5 = -\frac{\sigma_m r_0^2}{2G}.$$

Case II

This is similar to case I with the constants A_1 and A_5 having the following values.

(a) Permeable tunnel

$$A_1 = -\left(\frac{P_0}{\lambda + 2G}\right) \cdot \frac{1}{s} \cdot \frac{1}{\phi_1(r_0)}$$

$$A_5 = \left(\frac{p_0}{\lambda + 2G}\right) \cdot \frac{cr_0}{s^2} \cdot \frac{\psi_1(r_0)}{\phi_1(r_0)}$$

(b) Impermeable tunnel

$$A_1 = 0$$

$$A_5 = 0.$$

Case III

For this case it is clear $n = 2$, $\epsilon = 0$ and the solution which remains bounded as $r \rightarrow \infty$ is composed of three parts; solutions 1, 3 and 5. The constants A_1 , A_3 and A_5 are also obtained from the boundary conditions at $r = r_0$. The following expressions for A_1 , A_3 , A_5 may be verified.

(a) Permeable tunnel

$$A = \frac{1}{\chi} \cdot \left(\frac{\sigma_d}{2Gs}\right)$$

$$A_3 = \frac{1}{\chi} \cdot 4 \cdot \left(\frac{\sigma_d}{2Gs}\right) \cdot r_0^2 \cdot \left(\frac{\lambda + 2G}{2G}\right) \cdot \phi_1(r_0)$$

$$A_5 = \frac{1}{\chi} \cdot \left(\frac{\sigma_d}{2Gs} \right) \cdot r_0^4 \cdot \left\{ \left(\frac{c}{sr_0^2} \right) \cdot [2\phi_1(r_0) - r_0\psi_1(r_0)] \right. \\ \left. + \left(\frac{\lambda + 2G}{2G} \right) \cdot \phi_1(r_0) \right\}$$

$$\chi = \left(\frac{c}{sr_0^2} \right) \cdot [2\phi_1(r_0) + r_0 \cdot \psi_1(r_0)] + \left(\frac{\lambda + 2G}{2G} \right) \cdot \phi_1(r_0).$$

(b) *Impermeable tunnel*

$$A_1 = \frac{1}{\chi} \cdot 2 \cdot \left(\frac{\sigma_d}{2Gs} \right)$$

$$A_3 = \frac{1}{\chi} \cdot 2 \left(\frac{\sigma_d}{2Gs} \right) \cdot r_0^3 \cdot \left(\frac{\lambda + 2G}{2G} \right) \cdot \psi_1(r_0)$$

$$A_5 = \frac{1}{\chi} \cdot \left(\frac{\sigma_d}{2Gs} \right) \cdot r_0^4 \cdot \left\{ \left(\frac{c}{sr_0^2} \right) \cdot [2\phi_1(r_0) - r_0\psi_1(r_0)] \right. \\ \left. - \frac{1}{2} \cdot \left(\frac{\lambda + 2G}{2G} \right) \cdot r_0 \cdot \psi(r_0) \right\}$$

$$\chi = \left(\frac{c}{sr_0^2} \right) [2\phi_1(r_0) + r_0\psi_1(r_0)] - \frac{1}{2} \left(\frac{\lambda + 2G}{2G} \right) r_0\psi_1(r_0).$$

5. RESULTS

Explicit solutions for Cases I-III are now presented. Where it has not been possible to invert the Laplace transforms analytically they have been inverted numerically using eqn (16). In all cases the integrand has at most a simple pole at the origin and a branch line extending along the negative real axis and so it has been possible to take the path of integration C around the negative real axis.

Once the coefficients U_r , U_θ etc are known the corresponding values of the field quantities, i.e. u_r , u_θ , etc. at location (r, θ) and time t can be retrieved using expressions (13)

Case I

The solution in this case is independent of time, the drainage boundary condition at $r = r_0$ and the drained Poisson's ratio ν' . The coefficients of the field quantities are given by,

$$\left(\frac{2GU_r}{\sigma_m r_0} \right) = - \left(\frac{r_0}{r} \right)$$

$$\left(\frac{2GU_\theta}{\sigma_m r_0} \right) = 0$$

$$\left(\frac{P}{\sigma_m} \right) = 0$$

$$\left(\frac{S_{rr}}{\sigma_m} \right) = - \left(\frac{r_0}{r} \right)^2$$

$$\left(\frac{S_{\theta\theta}}{\sigma_m} \right) = \left(\frac{r_0}{r} \right)^2$$

$$\left(\frac{S_{r\theta}}{\sigma_m} \right) = 0.$$

Case II

If the boundary at $r = r_0$ is impermeable then the solution for Case II is trivial, i.e. $U_r = 0$, etc. This result does not hold if the boundary at $r = r_0$ is permeable. For the latter case only $U_\theta = S_{r\theta} = 0$. Isochrones for U_r and P are plotted in Figs. 2 and 3, where time has been expressed in a non-dimensional form, according to

$$T = \frac{ct}{r_0^2} = \left(\frac{k}{\gamma_w}\right) \cdot 2G \cdot \left(\frac{1-\nu'}{1-2\nu'}\right) \cdot \frac{t}{r_0^2} \tag{17}$$

When plotted in this form these results are independent of Poisson's ratio of the soil. The results in Fig. 2 indicate that for large times the magnitude of the radial displacement increases with increasing radius. This feature arises because of the nature of the boundary conditions adopted in the analysis. Specifically, it has been assumed that an indefinite amount of drainage of the pore water may occur at the tunnel boundary $r = r_0$. This is physically unlikely and so the displacement predictions at large times must be considered doubtful. Nevertheless, the results for small and moderate times are likely to be reasonable.

The results presented in Fig. 3 for the pore pressure coefficient P are in good agreement with solutions for the axi-symmetric diffusion (heat flow) problem that have been reported by Jaeger[3]. The pore pressure isochrones are approximately logarithmic functions of radius.

Values for the total stresses σ_{rr} and $\sigma_{\theta\theta}$ may be obtained from the results of Figs. 2 and 3 together with the following relations between u_r , p , σ_{rr} and $\sigma_{\theta\theta}$, which are valid for all times

$$\sigma_{rr} = 2G \frac{u_r}{r}$$

$$\sigma_{rr} + \sigma_{\theta\theta} = \left(\frac{\lambda + 2G}{2G}\right) p.$$

Case III

(a) *Permeable tunnel.* Solutions for the coefficients U_r , U_θ and P , corresponding to $\nu' = 0$, are shown in Figs. 4-6. Isochrones are again plotted for several values of non-dimensional time T . Isochrones for the stress coefficients S_{rr} , $S_{\theta\theta}$ are plotted in Figs. 7-9 for $\nu' = 0$. In the case of the total radial stress, Fig. 7, the variation with time of the stress distribution is very small. For the total circumferential stress there is a time dependency, with the largest variation occurring

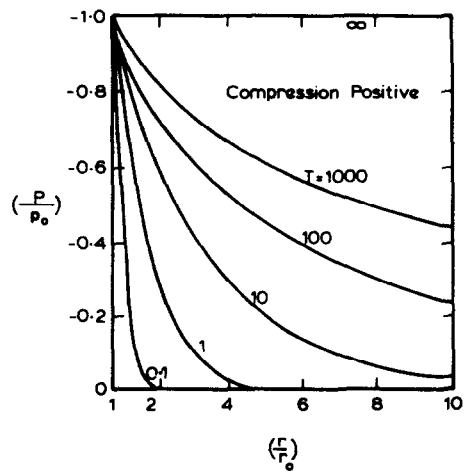
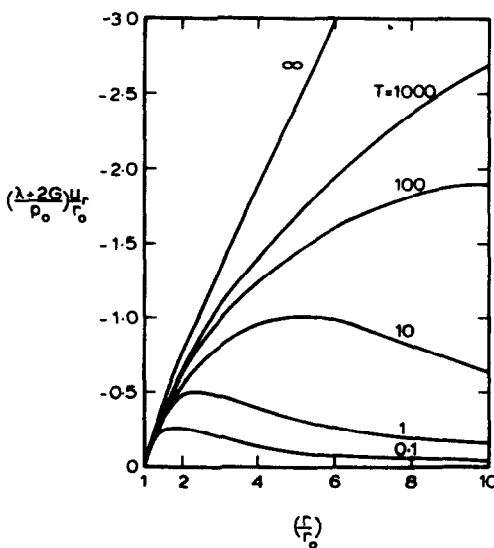


Fig. 2. Isochrones of radial displacement coefficient—Case IIa.

Fig. 3. Isochrones of excess pore pressure coefficient—Case IIa.

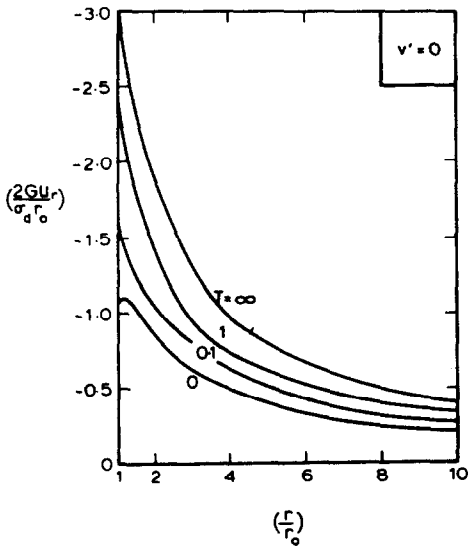


Fig. 4. Isochrones of radial displacement coefficient—Case IIIa

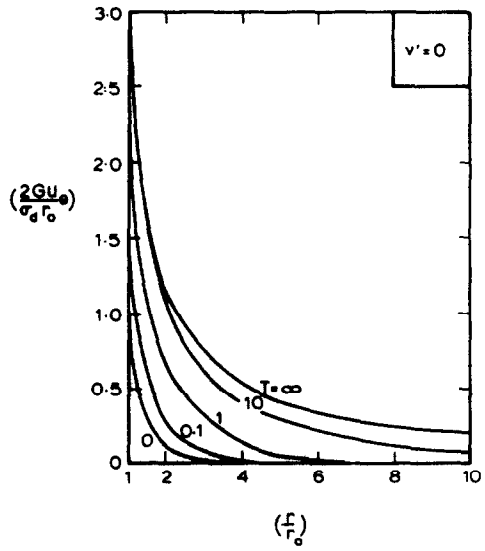


Fig. 5. Isochrones of circumferential displacement coefficient—Case IIIa.

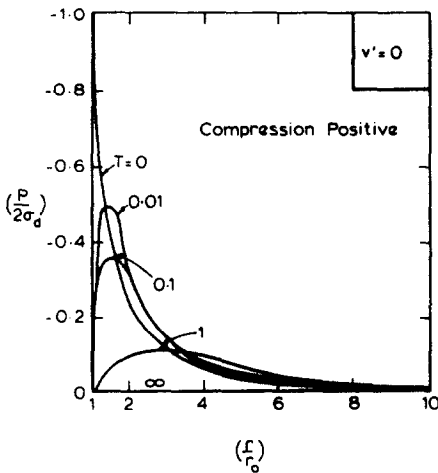


Fig. 6. Isochrones of excess pore pressure coefficient—Case IIIa

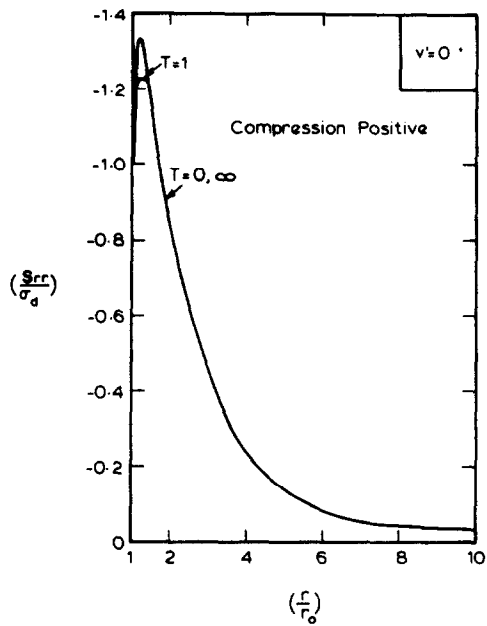


Fig. 7. Isochrones of total radial stress coefficient—Case IIIa.

at the tunnel boundary $r = r_0$, as shown in Fig. 8. For the shear stress distribution there also exists a variation with time; the largest variation occurring at about $T = 1$ as plotted in Fig. 9.

In general, the solutions for the Case IIIa tunnel problem are dependent on the value of Poisson's ratio ν' . Solutions for U_r , U_θ and P for a different soil, with $\nu' = 0.4$, are shown in Figs. 10 to 12. Results for the stress coefficients S_{rr} , $S_{\theta\theta}$ and $S_{r\theta}$ differ only slightly from those plotted in Figs. 7-9. The fully drained solutions for the stress coefficients are independent of

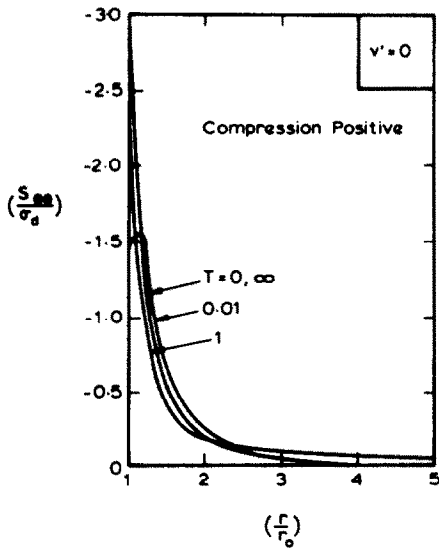


Fig. 8. Isochrones of total circumferential coefficient-Case IIIa.

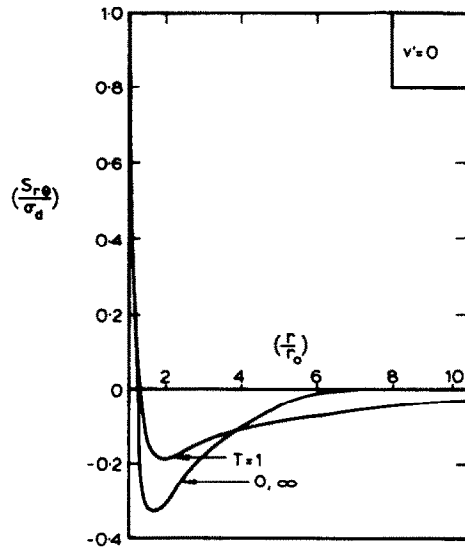


Fig. 9. Isochrones of shear stress coefficient-Case IIIa.

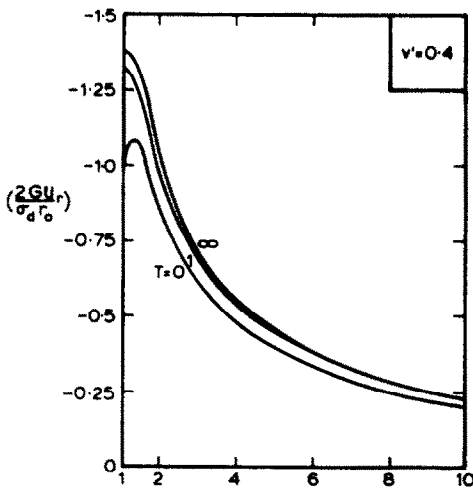


Fig. 10. Isochrones of radial displacement coefficient-Case IIIa.

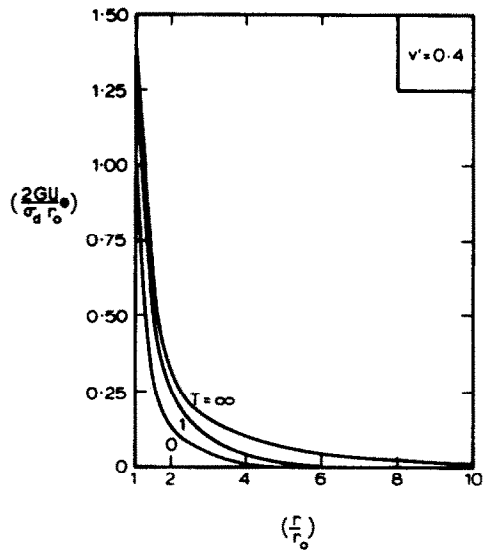


Fig. 11. Isochrones of circumferential displacement-Case IIIa.

Poisson's ratio and are given by

$$\left(\frac{S_{rr}}{\sigma_d}\right) = -4\left(\frac{r_0}{r}\right)^2 + 3\left(\frac{r_0}{r}\right)^4$$

$$\left(\frac{S_{\theta\theta}}{\sigma_d}\right) = -3\left(\frac{r_0}{r}\right)^4$$

$$\left(\frac{S_{r\theta}}{\sigma_d}\right) = -2\left(\frac{r_0}{r}\right)^2 + 3\left(\frac{r_0}{r}\right)^4.$$

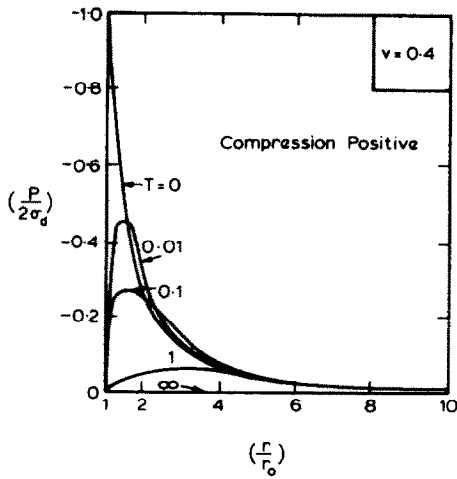


Fig. 12. Isochrones of excess pore pressure coefficient—Case IIIa.

(b) *Impermeable tunnel.* Selected results for the case of an impermeable tunnel wall (at $r = r_0$) are shown in Figs. 13–15, where isochrones for U_r , U_θ and P have been plotted for a soil with $\nu' = 0$. Some indication of the effects of the drainage boundary conditions may be gained from a comparison of these results with those of Figs. 4–6.

6. EXAMPLES OF SOLUTION SYNTHESIS

The results presented above were for the individual components of the consolidation problem; the breakdown into these components was described in Section 2. What remains is to assemble the components into a composite solution. In order to illustrate the assembly procedure three sets of values have been selected for the *in situ* stress state. In each example it has been assumed that the soil has a value of $\nu' = 0.4$ and a ratio of unit weights, $\gamma_w/\gamma = 0.5$. Three values have been selected for the earth pressure coefficient K_0 , viz. (a) $K_0 = 0.5$, (b) $K_0 = 1$, (c) $K_0 = 2$. Values such as these cover a range from normally consolidated clay through to over-consolidated clay. Using eqns (1) and (3) it has been possible to express all stress

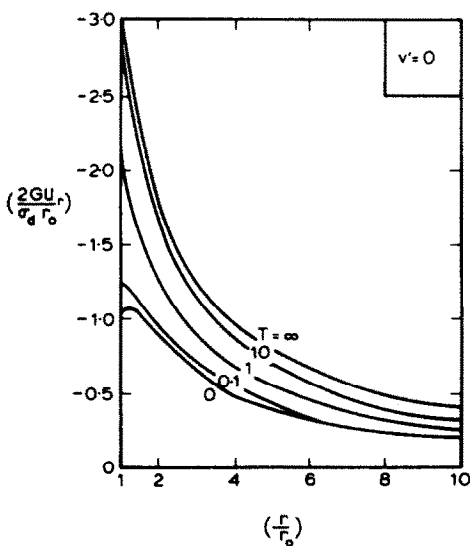


Fig. 13. Isochrones of radial displacement coefficient—Case IIIb.

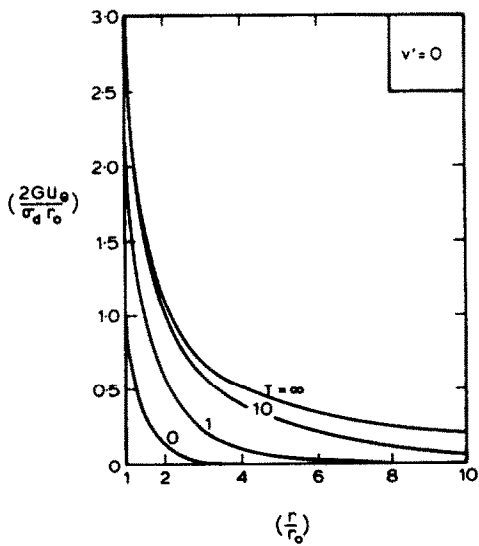


Fig. 14. Isochrones of circumferential displacement coefficient—Case IIIb.

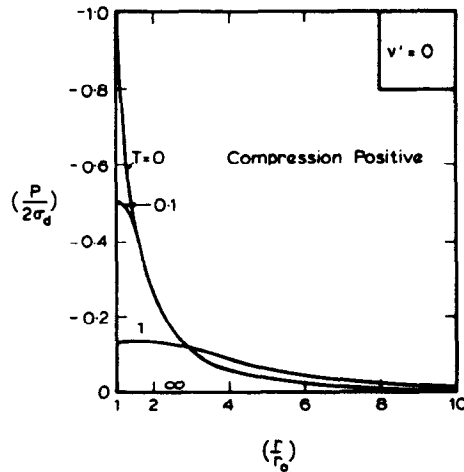


Fig. 15. Isochrones of excess pore pressure coefficient-Case IIIb.

quantities in terms of σ_v , the initial total overburden pressure. (σ_v is also an indicator of the depth at which the tunnel is bored.) The initial stress conditions are set out in Table 1.

Some results of the synthesis are presented in Table 2 for a tunnel with a permeable inner boundary. Results for the case of an impermeable tunnel are given in Table 3. Both tables show values for the displacements and stresses at selected times and at various locations around the tunnel wall (i.e. $r = r_0$ and selected values of θ). The *in situ* condition corresponds to $T = 0^-$; $T = 0^+$ corresponds to the instant immediately after the undrained deformation; and $T = \infty$ marks the end of consolidation.

In all of the examples the inner boundary at first "squeezes in" when the *in situ* stresses are removed, i.e. the tunnel opening becomes smaller during the infinitesimal time interval $T = 0^-$ to 0^+ . In example (b) the initial stress state is isotropic and so, when the boundary stresses are removed, the resulting displacements are symmetric. At the boundary ($r = r_0$) no additional movement occurs during the time interval $T = 0^+$ to ∞ (i.e. during consolidation), although consolidation movements will occur further out in the soil ($r > r_0$).

In examples (a) and (c) the displacements are not symmetric; in (a) the *in situ* vertical stress is bigger than the horizontal and thus the tunnel "squeezes in" more at the crown and invert ($\theta = 90^\circ, 270^\circ$) than at the spring line ($\theta = 0^\circ, 180^\circ$). As consolidation occurs the tunnel wall continues to move in at the crown and invert, but it moves back out at the spring line. The magnitudes of these consolidation movements are small when compared with the initial (undrained) displacements. For example (c) the pattern of movement is the reverse of that just described. The biggest inward movement occurs at the spring line since the *in situ* horizontal stress is bigger than the vertical component. During consolidation, inward movement continues at the spring line but outward movement occurs at the crown and invert.

Table 1. Initial stresses for example problems

Quantity	Example		
	(a)	(b)	(c)
$K_o = \sigma'_h / \sigma'_v$	0.5	1.0	2.0
$N = \sigma_h / \sigma_v$	0.75	1.0	1.5
σ_m / σ_v	0.875	1.0	1.25
p_o / σ_v	0.5	0.5	0.5
σ'_d / σ_v	-0.125	0	0.25

Table 2. Displacements and stresses at the permeable tunnel wall ($\nu' = 0.4$)

Quantity	Time	Example								
		(a) $K_o = 0.5$			(b) $K_o = 1.0$			(c) $K_o = 2.0$		
		θ^0			θ^0			θ^0		
		0	45	90	0	45	90	0	45	90
$\frac{2Cu_r}{\sigma_v r_o}$	0^-	0	0	0	0	0	0	0	0	0
	0^+	-0.75	-0.88	-1.0	-1.0	-1.0	-1.0	-1.51	-1.25	-0.99
	∞	-0.70	-0.88	-1.05	-1.0	-1.0	-1.0	-1.60	-1.25	-0.90
$\frac{2Cu_\theta}{\sigma_v r_o}$	0^-	0	0	0	0	0	0	0	0	0
	0^+	0	-0.13	0	0	0	0	0	0.26	0
	∞	0	-0.18	0	0	0	0	0	0.35	0
$\frac{\sigma_{rr}}{\sigma_v}$	0^-	0.75	0.88	1.0	1.0	1.0	1.0	1.5	1.25	1.0
	0^+	0	0	0	0	0	0	0	0	0
	∞	0	0	0	0	0	0	0	0	0
$\frac{\sigma_{\theta\theta}}{\sigma_v}$	0^-	1.0	0.88	0.75	1.0	1.0	1.0	1.0	1.25	1.5
	0^+	2.0	1.58	1.16	1.83	1.83	1.83	1.48	2.33	3.18
	∞	2.07	1.58	1.08	1.83	1.83	1.83	1.33	2.33	3.33
$\frac{\sigma_{zz}}{\sigma_v}$	0^-	0.75	0.75	0.75	1.0	1.0	1.0	1.5	1.5	1.5
	0^+	0.75	0.58	0.41	0.83	0.83	0.83	1.00	1.33	1.67
	∞	0.78	0.58	0.38	0.83	0.83	0.83	0.93	1.33	1.74
$\frac{\sigma_{r\theta}}{\sigma_v}$	0^-	0	0.13	0	0	0	0	0	-0.25	0
	0^+	0	0	0	0	0	0	0	0	0
	∞	0	0	0	0	0	0	0	0	0
$\frac{p}{\sigma_v}$	0^-	0.5	0.5	0.5	0.5	0.5	0.5	0.5	0.5	0.5
	0^+	0	0	0	0	0	0	0	0	0
	∞	0	0	0	0	0	0	0	0	0
$\frac{\sigma_{av}'}{\sigma_v}$	0^-	0.33	0.33	0.33	0.5	0.5	0.5	0.83	0.83	0.83
	0^+	0.92	0.72	0.52	0.89	0.89	0.89	0.83	1.22	1.62
	∞	0.95	0.72	0.49	0.89	0.89	0.89	0.75	1.22	1.69

Typically, it is found that 90% of the consolidation movement will occur during the time interval from $T = 0$ to about $T = 1$ for the permeable tunnel and during the interval $T = 0$ to about $T = 10$ for the impermeable tunnel. (For a tunnel of radius 2 m in a clay with $c = \text{lm}^2/\text{yr}$, this means that 90% of the consolidation movement of the wall will have taken place by about 4 yr after the tunnel is bored, if drainage is permitted at the inner boundary, and by about 40 yr if the tunnel walls are impermeable.)

The states of stress in the soil at various points around the inner boundary have also been tabulated at times $T = 0^-$, 0^+ and ∞ . It should be emphasised that all stress quantities presented are cumulative values, incorporating all changes which may have occurred up to the appropriate point in time. Nominally, all of the normal components are total stress values, however, in the case of the permeable inner boundary, the pore pressure is zero for times greater than $T = 0^-$. Hence for this case the values are also effective stresses for $T \geq 0^+$. In general, the total circumferential stress is increased at the instant the boundary stresses are removed. During consolidation some further though much smaller changes also occur.

For completeness the tables include values for the total stress component σ_{zz} which acts in the direction of the tunnel, i.e. perpendicular to the plane containing the circular opening. These values have been computed from the plane strain condition and a knowledge of the pore pressure changes.

Table 3. Displacements and stresses at the impermeable tunnel wall ($\nu' = 0.4$)

Quantity	Time	Example								
		(a) $K_0 = 0.5$			(b) $K_0 = 1.0$			(c) $K_0 = 2.0$		
		θ^0	θ^0	θ^0	θ^0	θ^0	θ^0	θ^0	θ^0	θ^0
	0	45	90	0	45	90	0	45	90	
$\frac{2Gu_r}{\sigma_v r_0}$	0 ⁻	0	0	0	0	0	0	0	0	0
	0 ⁺	-0.75	-0.88	-1.0	-1.0	-1.0	-1.0	-1.5	-1.25	-1.0
	∞	-0.70	-0.88	-1.05	-1.0	-1.0	-1.0	-1.6	-1.25	-0.9
$\frac{2Gu_\theta}{\sigma_v r_0}$	0 ⁻	0	0	0	0	0	0	0	0	0
	0 ⁺	0	-0.13	0	0	0	0	0	0.25	0
	∞	0	-0.18	0	0	0	0	0	0.35	0
$\frac{\sigma_{rr}}{\sigma_v}$	0 ⁻	0.75	0.88	1.0	1.0	1.0	1.0	1.5	1.25	1.0
	0 ⁺	0	0	0	0	0	0	0	0	0
	∞	0	0	0	0	0	0	0	0	0
$\frac{\sigma_{\theta\theta}}{\sigma_v}$	0 ⁻	1.0	0.88	0.75	1.0	1.0	1.0	1.0	1.25	1.5
	0 ⁺	2.25	1.75	1.25	2.0	2.0	2.0	1.5	2.5	3.5
	∞	2.25	1.75	1.25	2.0	2.0	2.0	1.5	2.5	3.5
$\frac{\sigma_{zz}}{\sigma_v}$	0 ⁻	0.75	0.75	0.75	1.0	1.0	1.0	1.5	1.5	1.5
	0 ⁺	0.99	0.75	0.51	1.0	1.0	1.0	1.19	1.5	1.98
	∞	0.95	0.75	0.55	1.0	1.0	1.0	1.10	1.5	1.90
$\frac{\sigma_{r\theta}}{\sigma_z}$	0 ⁻	0	0.13	0	0	0	0	0	-0.25	0
	0 ⁺	0	0	0	0	0	0	0	0	0
	∞	0	0	0	0	0	0	0	0	0
$\frac{p}{\sigma_v}$	0 ⁻	0.5	0.5	0.5	0.5	0.5	0.5	0.5	0.5	0.5
	0 ⁺	0.72	0.5	0.28	0.5	0.5	0.5	0.06	0	0.94
	∞	0.5	0.5	0.5	0.5	0.5	0.5	0.5	0.5	0.5
$\frac{\sigma_{av}'}{\sigma_v}$	0 ⁻	0.33	0.33	0.33	0.5	0.5	0.5	0.83	0.83	0.83
	0 ⁺	0.36	0.33	0.31	0.5	0.5	0.5	0.84	1.33	0.89
	∞	0.56	0.33	0.1	0.5	0.5	0.5	0.37	0.83	1.3

One particular quantity which has been tabulated and may be of some interest is the average effective stress $\sigma'_{av} = 1/3 (\sigma'_{rr} + \sigma'_{\theta\theta} + \sigma'_{zz})$. In all cases an overall increase in this mean stress occurs at the boundary as a result of instantaneous tunnel cutting. During the consolidation phase this mean stress may also vary, with the sign and magnitude of these additional changes varying with the initial stress condition (K_0) and with position around the tunnel (θ). Except for the soil in the region of the springline of example (c), the net result of tunnel cutting followed by consolidation is to cause an increase in mean effective stress at the inner boundary.

7. CONCLUSIONS

A method of analysis has been presented for the consolidation in an elastic soil due to the cutting of a long and deep circular tunnel. Solutions have been presented for the time dependent displacements and stress changes occurring in the soil surrounding the opening. No consideration has been given to the effects of introducing a tunnel lining or of creep and plastic flow within the soil. Such features are currently under investigation.

REFERENCES

1. A. M. Muir Wood, The circular tunnel in elastic ground. *Géotechnique* 25(1), 115-127 (1975).
2. M. J. Pender, Elastic solutions for a deep circular tunnel. *Géotechnique* 30(2), 216-222 (1980).
3. J. C. Jaeger, Numerical values for the temperature in radial heat flow. *J. Maths Phys.* 34, 316-321. (1956).

APPENDIX

The six independent solutions which are embodied in Equations (15) may be derived after consideration of the following four classes of problem.

- (a) Assuming $\Phi = \Omega = 0$ provides solutions 1 and 2.
- (b) Assuming $E_v = 0$ and $\Omega = \Phi$ provides solution 3 (for $n \neq 1$).
- (c) Assuming $E_v = 0$ and $\Omega = -\Phi$ provides solution 4 (for $n \neq -1$).
- (d) Assuming $E_v = \Omega = P = 0$ provides solutions 5 and 6.

The matrix M of eqn (15), which corresponds to these solutions is set out below.

$$M = \begin{bmatrix} \frac{c}{s} \psi_1 & \frac{c}{s} \psi_2 & \frac{1}{4} \left(\frac{n}{n-1} \right) r^{1-n} & \frac{1}{4} \left(\frac{-n}{n+1} \right) r^{n+1} & r^{-n-1} & r^{n-1} \\ -\frac{c}{s} \frac{n}{r} \phi_1 & -\frac{c}{s} \frac{n}{r} \phi_2 & \frac{1}{4} \left(\frac{n-2}{n-1} \right) r^{1-n} & \frac{1}{4} \left(\frac{n+2}{n+1} \right) r^{n+1} & r^{-n-1} & -r^{n-1} \\ \left(\frac{\lambda+2G}{2G} \right) \phi_1 & \left(\frac{\lambda+2G}{2G} \right) \phi_2 & \frac{1}{2} r^{-n} & -\frac{1}{2} r^n & 0 & 0 \\ -\frac{c}{s} \left(\frac{n^2}{r^2} \phi_1 - \frac{1}{r} \psi_1 \right) & -\frac{c}{s} \left(\frac{n^2}{r^2} \phi_2 - \frac{1}{r} \psi_2 \right) & \left(\frac{n}{4} + \frac{1}{2} \right) r^{-n} & \left(\frac{n}{4} - \frac{1}{2} \right) r^n & (n+1) r^{-n-2} & -(n-1) r^{n-2} \\ \left(1 + \frac{n^2}{r^2} \frac{c}{s} \right) \phi_1 - \frac{c}{s} \frac{1}{r} \psi_1 & \left(1 + \frac{n^2}{r^2} \frac{c}{s} \right) \phi_2 - \frac{c}{s} \frac{1}{r} \psi_2 & \left(-\frac{n}{4} + \frac{1}{2} \right) r^{-n} & -\left(\frac{n}{4} + \frac{1}{2} \right) r^n & -(n+1) r^{-n-2} & (n-1) r^{n-2} \\ -\frac{c}{s} \left(\frac{n}{r^2} \phi_1 - \frac{n}{r} \psi_1 \right) & -\frac{c}{s} \left(\frac{n}{r^2} \phi_2 - \frac{n}{r} \psi_2 \right) & \left(\frac{n}{4} \right) r^{-n} & -\left(\frac{n}{4} \right) r^n & (n+1) r^{-n-2} & (n-1) r^{n-2} \end{bmatrix}$$

where $\phi_1 = K_n \left(\sqrt{\frac{s}{c}} r \right)$, $\phi_2 = I_n \left(\sqrt{\frac{s}{c}} r \right)$, $\psi_1 = \sqrt{\frac{s}{c}} K_n' \left(\sqrt{\frac{s}{c}} r \right)$, $\psi_2 = \sqrt{\frac{s}{c}} I_n' \left(\sqrt{\frac{s}{c}} r \right)$, and I_n, K_n are the modified

Bessel functions of order n .